Molecular Crystals and Liquid Crystals

Publication details, including instructions for authors and subscription information:
http://www.tandfonline.com/loi/gmcl20

New Optical Nonlinear Material Based Upon PVA with PbS Quantum Dots

V. R. Lyakhovetsky [a], V. I. Volkov [a], A. A. Borshch [a], M. S. Brodyn [a], M. I. Strashnikova [a], V. Ya. Reznichenko [a], A. S. Kutsenko [b], S. M. Maloletov [b], S. Ya. Kuchmy [b] & F. Kajzar [c]

[a] Institute of Physics NASU, Kyiv, Ukraine

[b] Pisarzhevsky Institute of Physical Chemistry NASU, Kyiv, Ukraine

[c] CEA/Saclay, DRT/DECS, Gif sur Yvette Cedex, France

Version of record first published: 31 Aug 2006

To cite this article: V. R. Lyakhovetsky, V. I. Volkov, A. A. Borshch, M. S. Brodyn, M. I. Strashnikova, V. Ya. Reznichenko, A. S. Kutsenko, S. M. Maloletov, S. Ya. Kuchmy & F. Kajzar (2005): New Optical Nonlinear Material Based Upon PVA with PbS Quantum Dots, Molecular Crystals and Liquid Crystals, 426:1, 205-217

To link to this article: http://dx.doi.org/10.1080/15421400590891100

Mol. Cryst. Liq. Cryst., Vol. 426, pp. 205–217, 2005

ISSN: 1542-1406 print/1563-5287 online
DOI: 10.1080/15421400590891100

Taylor & Francis
Taylor & Francis Group

New Optical Nonlinear Material Based Upon PVA with PbS Quantum Dots

V. R. Lyakhovetsky
V. I. Volkov
A. A. Borshch
M. S. Brodyn
M. I. Strashnikova
V. Ya. Reznichenko
Institute of Physics NASU, Kyiv, Ukraine

A. S. Kutsenko
S. M. Maloletov
S. Ya. Kuchmy
Pisarzhevsky Institute of Physical Chemistry NASU, Kyiv, Ukraine

F. Kajzar
CEA/Saclay, DRT/DECS, Gif sur Yvette Cedex, France

High third-order nonlinear optical susceptibility ($\chi^{(3)}(\omega; \omega, -\omega, \omega) = -4{,}2 \times 10^{-16}(m^2/V^2)$). In the visible spectral range may be achieved in PVA composites containing narrow bad gap PbS semiconductor nanocrystals with a strong limitation of the area of charge carrier delocalization.

Keywords: composite material; lead sulfide nanoparticles; nonlinear optical effect

INTRODUCTION

Composite materials based on semiconductor (SC) nanocrystals (NC) and organic polymers have a number of unusual optical and electrophysical properties and are promising materials for applied optical electronics and nonlinear optics (NLO). In particular, due to the film-formation capabilities and ease of mechanical operation, these composites may be

Address correspondence to V. I. Volkov, Institute of Physics NASU, 46, Pr. Nauki, Kiev-28, 03650, Ukraine. Tel.: 8044265038, E-mail: volkov@iop.kiev.ua

used in the manufacture of light filters and various NLO elements. The major requirements for such materials are transparency, optical homogeneity, optical stability, and high NLO sensitivity.

NC dimensions less than one-fourth of the light wavelength provide the optical homogeneity of a composite, i.e., the lack of light scattering in the medium. The polymer matrix in the composite should be transparent in the given spectral region. Inorganic SCs have much greater optical stability than organic dyes which are commonly used as light-sensitive components of composites. Thus, the requirement of optical stability is transferred in composite systems with SC NC from the "guest" to the "host," i.e., to the polymer matrix. The optical stability of the polymer matrix is provided by a lack of photochemical reactions in the matrix. High NLO sensitivity is provided by localization of the excitation in the NC accompanied by a sharp increasing of the local electrical field under laser light excitation. Jind and Lind [1] have shown that the quantum limitation of an exciton appearing when the radius of SC particles is less than the exciton radius leads to the NLO sensitivity increasing. At the same time, Fukumi *et al.* [2] determined that the third-order NLO susceptibility $\chi^{(3)}$ of CdS nanocrystals under excitation by a laser light with $\lambda = 532\,\text{nm}$ was not increased when the diameter of CdS particles in a polymethyl methacrylate composite was decreased from 7.9 to 2.4 nm, but, on the contrary, decreased by a factor of about 1000. The authors did not explain this effect but it might be understood if one took into account that the spectral position of the laser radiation with $\lambda = 532\,\text{nm}$ was at the long-wave edge of the absorption band of the wide band gap CdS SC. Due to the quantum dimensional effect, the absorption spectrum is shifted toward shorter waves when the sizes of NC's are decreased. This reduces the absorption of the laser light and leads to a reduction of the NLO response of the material in question.

In the given work, we prepared a polymer composite with NC of a narrow band gap SC and measured the third-order NLO susceptibility of this composite. We selected lead sulfide as the narrow band gap SC because rather simple methods are known to exist for the synthesis of PbS nanoparticles and measurement of their mean size using X-ray structure analysis [3]. Polyvinyl alcohol (PVA) was used as a polymer matrix. Photochemical reactions do not occur in this polymer under the laser light irradiation at 532 nm. This provides the optical stability of the polymer matrix.

EXPERIMENTAL

Lead sulfide NCs were synthesized in an aqueous solution in the presence of PVA. A colloidal solution of PbS particles stabilized by PVA

together with the product of the substitution reaction (sodium nitrate, $Pb(NO_3)_2 + Na_2S \rightarrow PbS + 2NaNO_3$) was obtained by mixing and stirring the equimolar solutions of analytical-grade $Pb(NO_3)_2$ and Na_2S (supplied by Aldrich). Since the nascent sodium nitrate $NaNO_3$ prevents the formation of films of a satisfactory optical quality due to crystallization, this salt was removed from the solution by dialysis. It was observed that the absorption spectrum of the colloidal solution did not change during 10 days if the dialysis was carried out below 50°C. Meantime the edge of the absorption band shifted toward longer waves when the dialysis was carried out above 70°C indicating the increasing of the PbS particle size. The material thin films with thicknesses of 0.5, 1, and 2 μm were synthesized by the solution spreading onto the surface of 30×30-mm glass plates. The film thickness was varied in order to determine the optimal absorption of the light with $\lambda = 532\,\text{nm}$, at which the method for measuring the third-order NLO susceptibility, which we used, was the most sensitive.

X-ray structure analysis was performed using a DRON-4.07 diffractometer (CuK_α-radiation, $\lambda = 1.54178$ Å).

The thickness of our samples has been measured by means of a Linnik microinterferometer MII-4 using, for calculations, the difference of positions of the zero interference fringe at light reflectance from the film surface and the surface of the substrate.

The electronic absorption spectra were obtained by means of a spectrophotometer SF-20M.

The refractive index dispersion has been measured using a two-beam Jamin interferometer (Fig. 1) combined with a spectrograph DFS-13, whose reciprocal linear dispersion was equal to 4 Å/mm. The sample under study was placed in one shoulder of the interferometer. In such a case the pass difference between the two interfering beams equal to $[n_0(\lambda) - 1]\ell$ is arisen, where $n_0(\lambda)$ is the sample refractive index and l is the sample thickness. This pass difference leads to the interference pattern shift and in particular the zero fringe shift Δy. The relation between the position shift and the pass difference is determined by the expression

$$[n_0(\lambda) - 1]\ell = \left(\frac{\Delta y}{H}\right)\lambda, \tag{1}$$

where H is the interference fringe width. Registering the interference pattern with and without the sample we measured the zero interference fringe shift. Then we used this value to determine the refractive index of our sample. Thus the refractive index $n_0(\lambda)$ measuring technique is based on the direct measuring of the phase shift of a light wave passed through the sample.

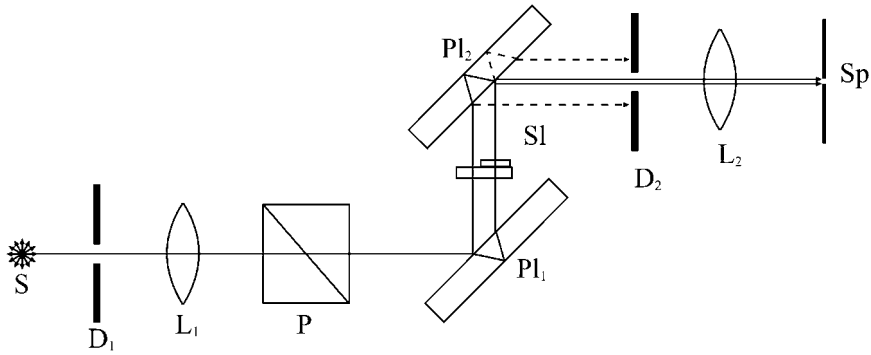

FIGURE 1 Experimental scheme for the refractive index dispersion $n_0(\lambda)$ measuring. A Jamin interferometer is combined with a spectrograph: S is the light source, D_1 and D_2 are the diaphragms, L_1 and L_2 are the lenses, P is the polarizer, Pl_1 and Pl_2 are the Jamin interferometer plates, Sl is the sample on a glass substrate placed in the interferometer, Sp is the spectrograph slit.

The nonlinear refraction in the samples was studied by the dynamic holographic grating recording in the scheme of degenerate two-wave mixing (Fig. 2a). A one-mode frequency-doubled YAG:Nd^{+3} laser ($\tau = 10$ ns, $\lambda = 532$ nm, TEM_{00}) was used as a light source. The time resolution of our registering system was about 10 ns. The read out of the dynamic gratings was carried out using a cw He-Ne laser. The interference field of the two interacting coherent light beams from the pulsed laser induced a dynamic grating in the sample based on the refractive index modulation, on which the self-diffraction of recording beams was observed. The dynamic gratings were recorded on the basis of the third-order optical nonlinearity characterized by the nonlinear optical susceptibility $\chi^{(3)}(\omega;\ \omega,\ -\omega,\ \omega)$. The value of $\chi^{(3)}(\omega;\ \omega,\ -\omega,\ \omega)$ was evaluated by means of diffraction efficiency of the recorded gratings measurements using the equation [4]

$$|\chi^{(3)}(\omega)|\left[\mathrm{m}^2/\mathrm{V}^2\right] = \frac{4}{3}\varepsilon_0 \mathrm{c} n_0^2 n_2 = \frac{4\varepsilon_0 \mathrm{c} n_0^2 \lambda\sqrt{\eta}}{3\pi\ell \mathrm{I}_0}, \qquad (2)$$

where n_0 is the refractive index of a sample, n_2 is the nonlinear refractive index coefficient, l is the sample thickness, I_0 is the total intensity of the recording light, λ is the light wavelength, η is the diffraction efficiency, c is the speed of light, and ε_0 is the absolute dielectric constant of a vacuum. The sign of the refractive index nonlinear change was determined using data obtained by the Z-scan technique (Fig. 2b).

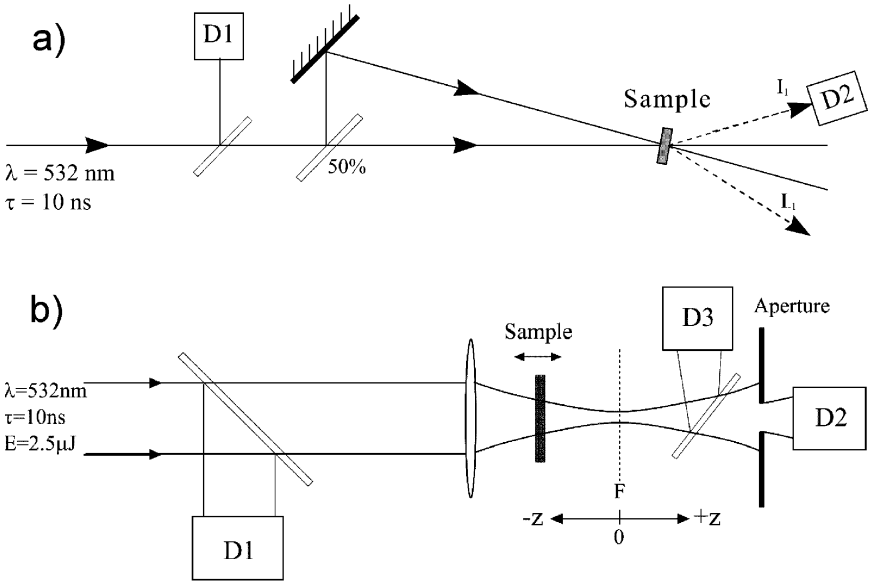

FIGURE 2 Experimental setup for: a) degenerate four-wave mixing (self-diffraction) and b) nonlinear lens technique whose particular modification is known as an Z-scan. $D_{1,2,3}$ are detectors.

RESULTS AND DISCUSSION

Determination of Particle Sizes

It is known that the NC size decrease leads to a broadening of X-ray diffraction peaks. The diffractogram presented in Figure 3 demonstrates the influence of a PbS NC size on the broadening of the diffraction peaks at $2\theta = 26.1$; 30.2; 43.06; and 50.6. The vertical lines give the position of various lines of bulk PbS. It is seen that our samples have the same pattern, though the maxima are slightly shifted in our case toward higher 2θ values. The peak at $2\theta = 19$ corresponds to PVA. The broadening of diffraction peaks relatively to the peaks of a reference monocrystal sample with the half width B_S makes it possible to define the NC size. The silicon monocrystal with $B_S = 0.38^\circ$ was used as a reference sample. The peak broadening $\Delta = (B^2 - B_S^2)^{1/2}$ is related to the particle mean diameter 2 R by the Sherrer's equation

$$2R = \frac{K\lambda}{\Delta \cdot \cos\vartheta}, \tag{3}$$

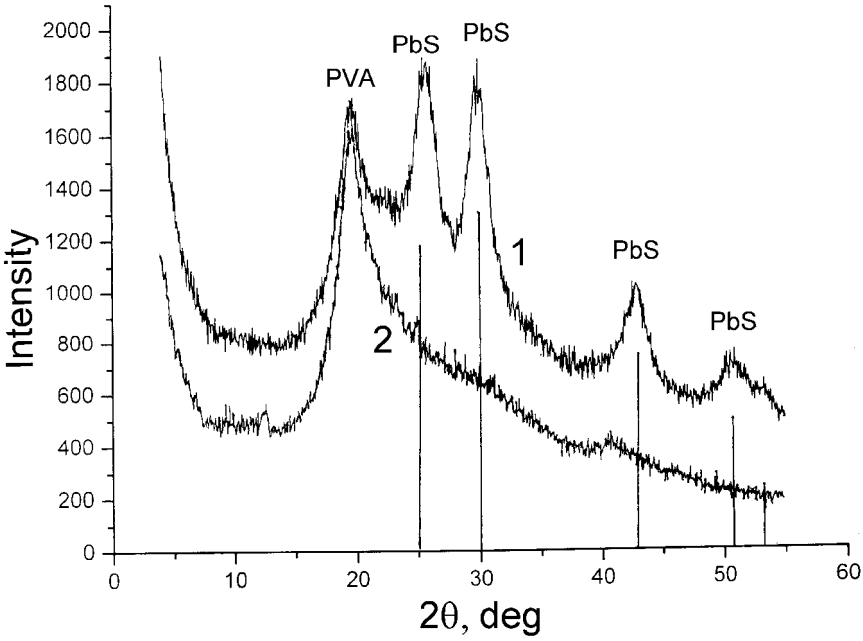

FIGURE 3 X-ray diffraction pattern: (1) – PVA/PbS composite film 4 vol.% of 5 nm PbS particles) and (2) – pure PVA film. The vertical lines indicate the positions of various lines of bulk PbS.

where $\lambda = 1{,}542$ Å is the X-ray wavelength, θ is the scattering angle, Δ is the halfwidth of the diffraction peak in units of 2θ, K is the geometric factor taken to be 1 for the cubic rock-salt structure of PbS.

Applying Eq. (1) to our X-ray diffraction pattern presented in Figure 3, we calculated that the mean radius R of PbS NC in our samples was ≈ 2.5 nm.

Determination of Band Gaps

According to the hyperbolic zone model [3], the band gap of PbS SC particles with radius R is given by the equation

$$E_g^* = \left[E_g^2 + \frac{2\hbar^2}{m^*}\left(\frac{\pi}{R}\right)^2 E_g\right]^{1/2}, \tag{4}$$

where $1/m^* = 1/m_e^* + 1/m_h^*$ and m_e^* and m_h^* are the effective electron and hole masses in SC, $\hbar$ is the Planck constant, and E_g is the band gap of the bulk SC.

For our PbS nanoparticles, $E_g = 0.41\,eV$, $m^* = 0.085\,m_e$ [3] (m_e is the free electron mass), and $R = 2.5\,nm$. Using these parameters and formula (4), we obtained that the band gap $E_g^* = 1.05\,eV$. In that case, the dimension-dependent increase of the band gap width of PbS NC that is the quantum dimensional effect is $\Delta E_g = E_g^* - E_g = 0.64\,eV$.

The absorption spectrum of a film of the composite material PVA/PbS made from the solution of PbS with a concentration of 10^{-2} mol/l and PVA with 1 mass% concentration is shown in Figure 4. The concentration of 5-nm PbS NCs in the film was 4 vol%. The thickness of the film was measured using a Linnik microphotometer MII-4 and was 1 μm. In comparison with the spectra of bulk lead sulfide samples [3], the edge of the absorption band of the PbS NC's is shifted toward shorter waves by about 2300 nm. This spectral shift in our composite is the result of the quantum dimensional effect. The vertical line in the IR spectral range at $\lambda = 1180\,nm$ indicates the position of the energy band gap of PbS nanoparticles, $E_g^* = 1.05\,eV$, calculated using formula (4). It is in a fairly good agreement with the value of E_g^* obtained from the fundamental absorption edge of PbS nanoparticles. The vertical line in the visible spectral range in Figure 4 shows the position of the exciting light wavelength $\lambda = 532\,nm$. The optical density of the film under study was 0.3 at 532 nm and the correspondent transmission of the laser light was about 50%.

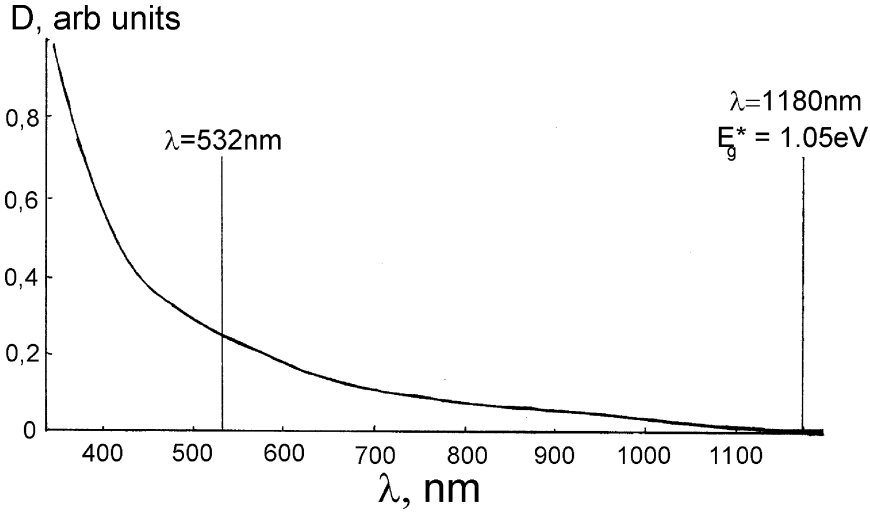

FIGURE 4 Absorption spectrum of the PVA/PbS composite film (4 vol% of 5 nm PbS) with a thickness of 1 μm.

The value of the composite refractive index for the excitation wavelength $n_{0(\lambda=532\,nm)}$ which is necessary for calculation of the optical nonlinear susceptibility $\chi^{(3)}(\omega; \omega, -\omega, \omega)$ using Eq. (2) may have intermediate number between $n_0 = 1.5$ for PVA and $n_0 = 4.3$ for PbS depending upon PbS NC concentration. In addition, it has experimentally been shown in [5] that the refractive index of a composite polymer material containing PbS NC is influenced by the quantum dimensional effect. The refractive index of the material with PbS particles less than 20 nm is vividly decreased with the size of particles and, when the size of particles reaches some nm, n_0 of such a composite material almost does not differ from the refractive index of the polymer matrix.

We have measured the refractive index dispersion $n_0(\lambda)$ for our composite material in the visible spectrum range. The method is based on the direct measuring of a phase change of the light wave having passed through the sample. Figure 5 shows the dependence $n_0(\lambda)$. One can see from the figure that the dependence of n_0 on λ is not significant, n_0 at $\lambda = 532$ nm being equal to 1.87 which is 0.37 higher than the refractive index of PVA.

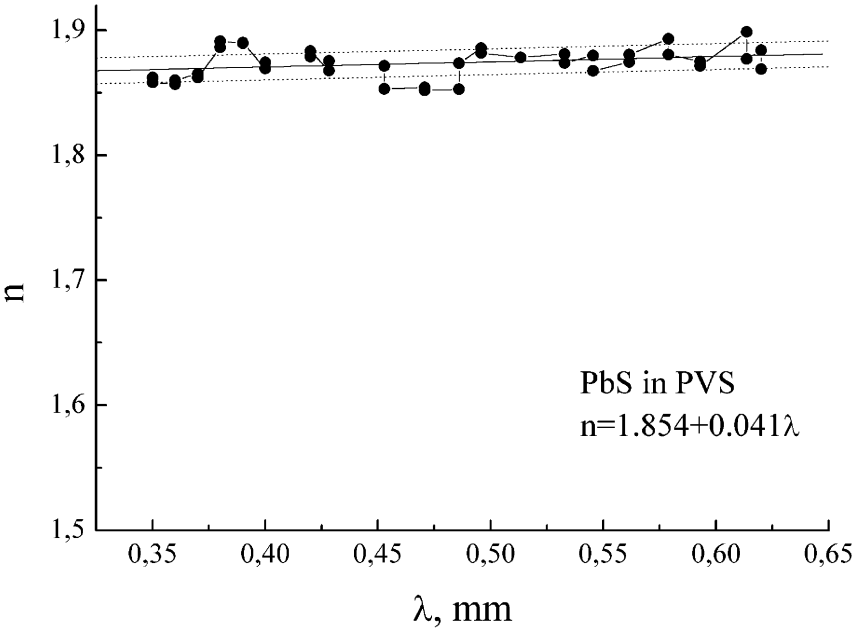

FIGURE 5 Refractive index dispersion of the PVA/PbS nanocomposite.

In the sample with the thickness of 1 μm, we managed to write phase dynamic gratings with the response time less than 10 ns in the scheme of degenerate two-wave mixing. That is, our composite material exhibits the strong and fast nonlinear refraction.

Using the experimental data $n_{0(\lambda=532\,nm)} = 1.87$, $l = 1$ μm, $\lambda = 0.53\,\mu m$, $I_0 = 7 \cdot 10^9\,Wm^2$, and $\eta = 3 \cdot 10^{-6}$, we obtained $\chi^{(3)}(w) = (4.2 \pm 2.1) \cdot 10^{-16}\,m^2/V^2$. For comparison, Table 1 gives the literature data on $\chi^{(3)}(\omega)$ obtained for some composites and other materials. This table shows that the cubic NLO susceptibility for the polymer composite with PbS NC exceeds the corresponding value for both reported bulk NLO materials and a series of composites with different NC. Some parameters of bulk and polymer materials containing NC of SC CdS and PbS of similar dimensions are given in Table 2 for comparison of the quantum dimensional effect and the third-order NLO sensitivity of composites with wide band gap SC (CdS) and narrow band gap SC (PbS). The Bohr radius of an exciton for bulk CdS and PbS SC was estimated using the well-known equation

TABLE 1 Third-Order Nonlinear Optical Susceptibility of Some Materials

Material	Size of nanocrystals 2R, nm	NLO index of material Re[$\chi^{(3)}$], m^2/V^2	λ, nm	Reference
PbS in PVA	5	$(-4.2 + 2.1) \cdot 10^{-16}$ ($n_0 = 1.87$)	532	Our data
CdS_xSe_{1-x} in glass				
"Corning N3484"		$1.8 \cdot 10^{-16}$	532	[1]
"Corning N2434"		$7 \cdot 10^{-17}$	580	[1]
"Schott RG 685"		$4.2 \cdot 10^{-17}$	694.3	[1]
GaAs m glass "Vycor"	5	$-3.4 \cdot 10^{-18}$ ($n_0 = 1.5$)	1064	[10]
CdS in PMMA	7.9	$2.2 \cdot 10^{-19}$	532	[2]
CdS in PMMA	6.2	$8.7 \cdot 10^{-20}$	532	[2]
CdS in PMMA	2.4	$<1.4^{-22}$	532	[2]
Cd (Se.Te) in glass "Hoya 720"	$3.5 \div 6$	10^{-22}	1064	[11]
GaAs	Bulk	$-1.3 \cdot 10^{-18}$	1064	[10]
CdS	Bulk	$-7 \cdot 10^{-19}$	610	[6]
CdTe	Bulk	$-6.4 \cdot 10^{-19}$	1064	[12]
ZnTe	Bulk	$2.5 \cdot 10^{-19}$	1064	[12]
ZnSe	Bulk	$-1.3 \cdot 10^{-19}$	532	[12]
CS_2	Liquid	$1.7 \cdot 10^{-20}$		[2]

Note. To prepare this table, we used the formula $\chi^{(3)}$ $[m^2/V^2] = 2.65 \cdot 10^{-7} n_0 n_2$ $[cm^2/W]$, where n_0 and n_2 are the linear and nonlinear refractive indices of the material: $\chi^{(3)}$ $[m^2/V^2] = 1.396610^{-8}\chi^{(3)}$ [esu].

TABLE 2 Some Parameters of Bulk CdS and PbS and Polymer Composites with CdS and PbS Nanocrystals

	Bulk semiconductor					Polymer material with semiconductor nanocrystals		
Semiconductor	E_g, eV	ε	m^*	r_{ex}, nm	R, nm	R_{part}, nm	ΔE_g, eV	$\chi^{(3)}(\omega)$, m^2/V:
CdS	2.5 [8]	5.5 [8]	0.172 [9]	1.7	2.5 ÷ 3 [7]	1.7 [2]	0.45 [8]: 0.42 [9]	$<2\cdot10^{-22}$ [2]
PbS	0.41 [3]	17.2 [3]	0.085 [3]	10.7	9[7]	2.5	0.64	$4.2\cdot10^{-16}$

Note. R is the nanocrystal radius, below which the quantum dimensional effect appears.

$$r_{ex} = \frac{\hbar^2 \varepsilon}{e^2}\left(\frac{1}{m_e^*} + \frac{1}{m_h^*}\right), \tag{5}$$

where ε is the optical dielectric constant of the SC, e is the electron charge.

Vossmeyer *et al.* [9] have noted that the quantum dimensional effect starts to appear for CdS particles with radius R_{part} less than 2.5–3 nm, while this effect starts to appear for PbS particles with R_{part} less than 9 nm. These results are in satisfactory agreement with our data regarding the exciton radius for these SC: $r_{ex(CdS)} = 1.7$ nm, $r_{ex(PbS)} = 10.7$ nm (the parameters required for these calculations are given in Table 2). The obtained high value of $r_{ex(PbS)}$ is mainly a result of the high dielectric constant.

There are different explanations for the origin of the nonlinearity of the optical properties of composites with SC NC involving thermal, photoisomerization, electrostriction, and electronic mechanisms. The $\chi^{(3)}$ value for SC NC with particle size R_{part} less than r_{ex} is determined by electrons and not by excitons as in bulk SC [13]. The experimental method described above allows us to observe the fast NLO response ($\tau \leq 10$ ns) due to the most rapid and practically important electronic mechanism. This mechanism is divided into several types depending on the NC dimensions [13].

A classification of types of the spatial limitation of exciton and charge carriers relatively to the size of SC NC was given in [14]. Machol *et al.* [15] related PbS NC with a radius of 2 nm to the case of strong charge carrier limitation. The size of our PbS nanoparticles is close to that in the work by Machol [15] and four times less than

the exciton radius for bulk PbS (see Table 2). In addition, it has been pointed out in [16] that the radii of an electron $r_e = \varepsilon\hbar^2/m_e^* e^2$ and a hole $r_h = \varepsilon\hbar^2/m_h^* e^2$ are the same in PbS. In our case, $r_e = r_h = 5.35\,\text{nm}$. nm. Thus, the size of PbS NC in our material is two times less than the radii of an electron and a hole in PbS. This suggests that the electronic mechanism for optical nonlinearity for our composite should be assigned to the case of the smallest NC, in which there is a considerable spatial limitation of charge carriers, i.e., $R_{part} < r_e,\ r_h$. In this case, the electron and hole energy spectrum is quantized, and the occupation of discrete levels leads to large values of NLO susceptibility $\chi^{(3)}$ [13].

The results of Z-scan measurements carried out on our sample are shown in Figure 6. It is seen from the figure that the nonlinear refractive index coefficient is negative ($n_2 < 0$). In [17], the authors have also observed the negative sign of a nonlinear refractive index change at $\lambda = 780\,\text{nm}$ in a composite with 5-nm PbS NC. The negative sign of the refractive index change observed in our material can be attributed to the contribution of nonequilibrium free carriers generated in PbS NC under excitation.

The dimensions of the CdS and PbS NCs in the composites given in Table 2 are much less than the corresponding radii of excitons in these bulk SCs. This may account for the strong quantum dimensional and NLO effects for PbS NC (see Table 2).

However, it is difficult to attribute the enormous differences in the third-order nonlinear optical susceptibility for composites with PbS and CdS nanocrystals $\left[\chi^{(3)}_{PbS}/\chi^{(3)}_{CdS} \approx 10^6 (\text{see Table1})\right]$ only to the merely approximately one-and-a-half-fold discrepancy between the greater dimension-dependent forbidden band gap of PbS nanocrystals and the corresponding value of CdS nanocrystals (Machol *et al.* [15] proposed that this ratio is only about 10^3). Such a result for the composite with CdS nanocrystals may be attributed to the large drop in the absorption of the laser beam at $\lambda = 532\,\text{nm}$ due to the dimension-dependent shift of the absorption spectrum toward shorter waves. In the case of PbS nanocrystals, we showed that the use of narrow band gap semiconductor made it possible to choose the nanocrystal radii, which, on the one hand, were much less than the exciton radius of the bulk semiconductor and, on the other hand, provided the absorption of the laser light beam by the sample required for achieving large nonlinear optical responses. This comparison demonstrates the advantage of nanocrystals of narrow band gap semiconductors such as PbS over wide band gap semiconductors such as CdS when they are used in composites for nonlinear optics in the visible spectral range.

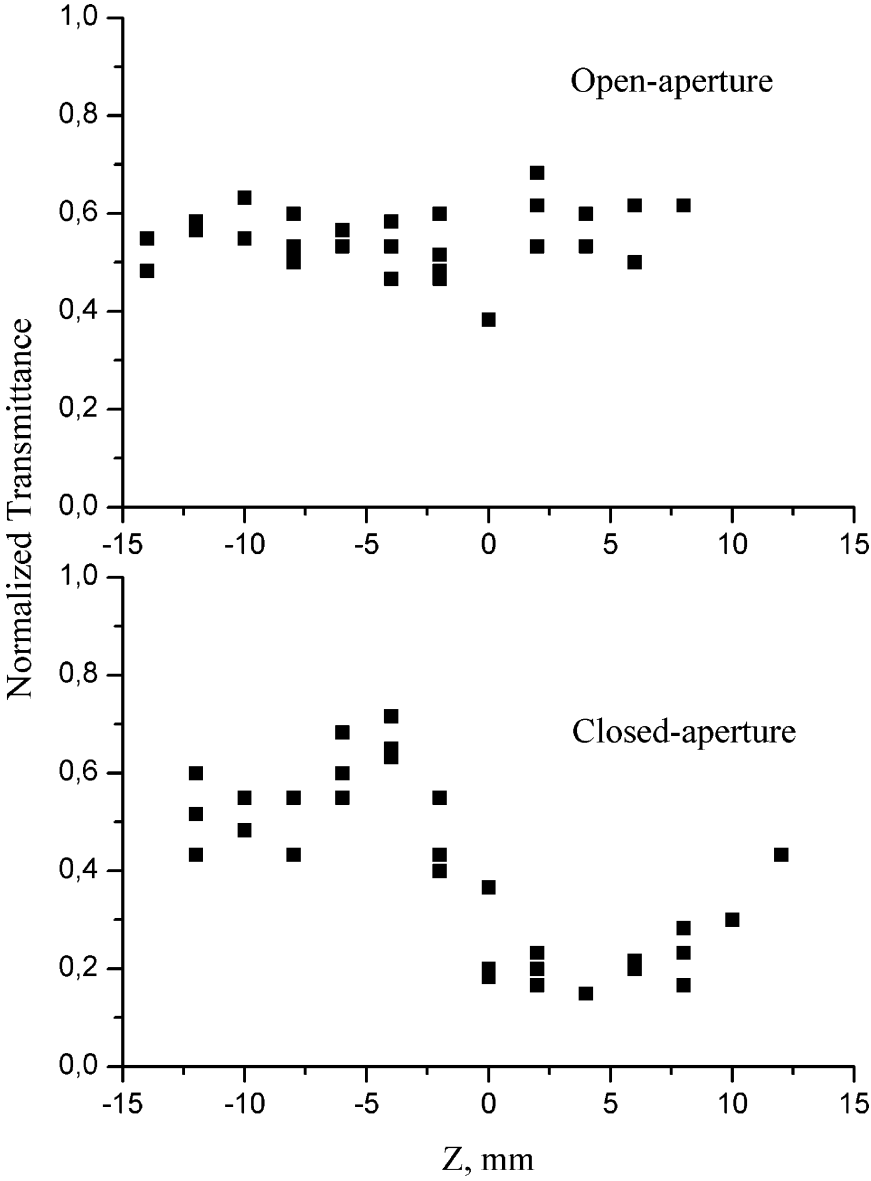

FIGURE 6 Z-scan traces.

Thus, our results show that high third-order nonlinear optical susceptibility values in the visible spectral region may be achieved in polymer composites with nanocrystals of a narrow band gap

semiconductor with a strong limitation of the area of charge carrier delocalization.

REFERENCES

[1] Jind, R. K. & Lind, R. C. (1983). *J. Opt. Soc. Am.*, *73*(5), 647–653.
[2] Fukumi, T., Skaguchi, T., Yanagida, S., & Euokida, T. (1992). In: *Nonlinear Optical Materials*. Boca Raton, Ann Arbor, (Eds.), CPC Press: London, 115–120.
[3] Wang, J., Suna, A., Mahler, A., & Kasowski, R. (1987). *J. Chem. Phys.*, *87*(12), 7315–7322.
[4] Byrne, H. J. & Blau, W. (1990). *Synth. Meth.*, 37(1/3), 231–247.
[5] Kyprianidou-Leodidou, T., Caseri, W., & Suter, U. W. (1994). *J. Phys. Chem.*, *98*(36), 8982–8991.
[6] Beecroft, L. L. & Ober, C. K. (1997). *Chem. Mater.*, *9*(6), 1302–1317.
[7] Wang, Y. & Herron, N. (1991). *J. Phys. Chem.*, *95*(2), 525–532.
[8] Wang, Y. & Herron, N. (1990). *Phys. Rev. B*, *42*(1), 7253–7255.
[9] Vossmeyer, T., Katsikas, L., Giersig, M. *et al.* (1994). *J. Phys. Chem.*, *98*(31), 7665–7673.
[10] Justus, B. L., Tonucci, R. J., & Berry, A. D. (1992). *Appl. Phys. Lett.*, *61*(26), 3151–3153.
[11] Cotter, D., Burt, M. G., & Manning, R. J. (1992). *Phys. Rev. Lett*, *68*(8), 1200–1203.
[12] Said, A. A., Sheik-Bahae, M., Hagan, D. J. *et al.* (1992). *J. Opt. Soc. Am. B*, *9*(3), 405–414.
[13] Venger, E. F., Goncharenko, A. V., & Dmitruk, M. L. (1999). *Optics of Small Particles and Dispersed Media* [in Ukrainian], Naukova Dumka, Kiev.
[14] Efros, A. A., & Efros, A. L. (1982). *Fiz. Tekhn. Poluprov.*, *16*(7), 1209–1214.
[15] Machol, J. L., Wise, F. W., Patel, R. C., & Tanner, D. B. (1993). *Phys. Rev. B*, *48*(3), 2819–2822.
[16] Kang, T. & Wise, F. M. (1997). *JOSA B*, *14*(17), 1632–1636.
[17] Lin, B., Li, H., Chew, C. H., Que, W., Lam, Y. L., Kam, C. H., Gan, L. M., & Xu, G. Q. (2001). *Materials Letters*, *51*(6), 461–469.